ISABE-2015-20203

Configuration Options for High-Power, Low Weight Aerospace Superconducting Distributed Propulsion Cryocoolers

Joseph Palmer, Meletis Pagonis, and Peter Malkin
Cranfield University
Department of Power and Propulsion
Cranfield, Bedfordshire, MK43 0AL, UK

Abstract

Distributed propulsion coupled with superconducting technology potentially offers numerous advantages over present day aircraft propulsion. Superconducting technology however requires cryogenic cooling systems in order to function normally. Cryogenic cooling systems are typically bulky, heavy, and inefficient. Although future improvements could go some way to mitigate the issues surrounding cryogenics, configuration choices must be examined in detail for potential advantageous design decisions that could be applied. This paper has examined two variables for cryogenic cooling systems; temperature of operation, and cryocooler configuration used. It was found that temperature has a significant impact on the overall mass and power of a cryogenic cooling system. Furthermore, it was also found that configuration does not impact power, but does impact the mass of a given concept. The conclusions of the paper are that future superconducting materials must be examined in more detail, and that larger aircraft will see increasing benefits from developments in cryogenic technology over smaller aircraft.

Glossary

ATRU – Auto-Transformer Rectifier Unit
BSCCO – Bismuth Strontium Calcium Copper Oxide
BWB – Blended-Wing Body
DEAP – Distributed Aerospace Electrical Propulsion
ECS – Environmental Control Systems
ICS – Icing Control System
LNG – Liquid Natural Gas
MgB_2 – Magnesium Diboride
RBC – Reverse-Brayton Cryocooler
SEA – Superconducting Electric Aircraft
TeDP – Turbo-electric Distributed Propulsion
TRL – Technology Readiness Level
TRU – Transformer Rectifier Unit
VFSG – Variable Frequency Superconducting Generator
YBCO – Yttrium Barium Copper Oxide

Introduction

Novel approaches to aircraft propulsion and power distribution are being considered by the aviation industry, driven by increasing fuel costs and growing industrial competition. Electrically distributed propulsion potentially offers a number of advantages over gas turbines, such as freedom of propulsor placement and greater control and flight cycle management capability (Kim, 2010). Recent studies have shown that in order for electrically distributed propulsion to become viable and competitive with current gas turbine technology, the power density of machines and efficiency of power distribution networks must improve (Berg *et al*, 2015, Green, Schiltgen, and Gibson, 2012).

Superconductivity potentially offers the solution to performance issues encountered. Superconducting materials are able to carry orders of magnitude more energy than conventional conductors per unit weight, and are also highly efficient due to zero resistance when using DC power (Malkin and Pagonis, 2015). There is however a caveat to superconducting materials; they require cooling to cryogenic temperatures in order to function normally.

Cryogenic cooling technology has been identified in recent studies by (Berg *et al*, 2015) and (Palmer and Shehab, 2015) as a key technological obstacle to overcome towards realization of a superconducting electrical network on board aircraft. The prime movers for its criticality are weight and required input power. Studies by Palmer and Shehab (2015) have shown that the most viable thermodynamic concept for cryocooling is likely to be the RBC. Furthermore, the most critical components have been identified; compressors, turbines, and heat exchangers must all show some level of improvement over the current level of technology if goals outlined by Kim (2010) are to be realized.

Figure 1 shows the performance past and predicted for aerospace cryocoolers. The graph was generated by collecting aerospace cryocooler examples already in existence, and applying the mass estimation tool developed in previous studies to proposed power levels of future superconducting networks (Palmer and Shehab, 2015). This paper explores a different approach to the problem using models derived for the DEAP project, jointly undertaken by Airbus Group Innovations, Rolls-Royce plc, and Cranfield University. The paper explores whether selected design decisions in a set of proposed superconducting networks can result in performance improvements, particularly on the overall final weight and input power metrics of cryogenic cooling systems.

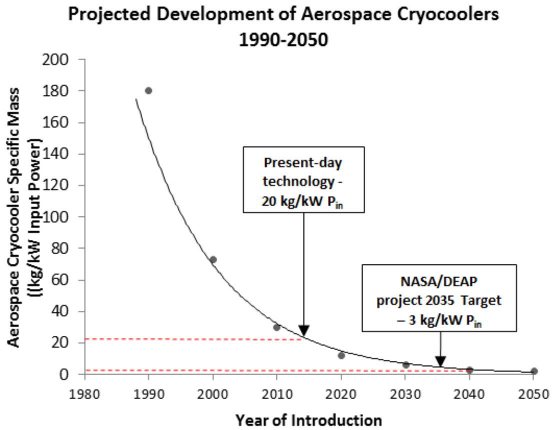

Figure 1 Projected development of aerospace cryocoolers

Two concepts are explored; the first is a superconducting electrical network for the purposes of propulsion, and the second is a superconducting network for the purposes of power distribution. In each case, three hypothetical examples are given, and existing models are used to determine the weight and input power required for each example. The key outcome of the paper is to investigate what impact the high-level architectural choices in terms of propulsion and power distribution will have on cryogenic cooling systems, and whether improvements can be made to a cryogenic cooling system performance by intelligent consideration of superconducting network temperature architecture.

Concept Aircraft Background and Architectures

Figure 2 NASA N3-X concept aircraft

At the time of writing, two major commercial aviation concept aircraft are considering using superconducting electrical propulsion systems. NASA's N3-X concept is the first such example. The N3-X uses a superconducting network to distribute power from four superconducting generators to 14 superconducting motor-driven fans spread along the trailing edge of the blended-wing body (BWB) airframe (Figure 2, Felder, Brown, and Kim, 2009). The total installed electrical power is around 80 MW. The concept outlines two potential candidate superconducting materials, MgB_2 and BSCCO (Felder, Brown, and Kim, 2009). The key difference between these two concepts will be cooling configuration; MgB_2 has a critical temperature (T_c) of 39 K, while the BSCCO superconductor has a higher T_c of 90-110 K (Ekin, 2006). Practical operating temperatures for each of these materials are 20 K and 65 K respectively (Larbalestier *et al*, 2001). NASA have specified that the MgB_2 concept would be cooled using liquid hydrogen as the heat sink, negating the need for cryocooling equipment, whereas the BSCCO concept would be cryocooled using RBC cryocoolers.

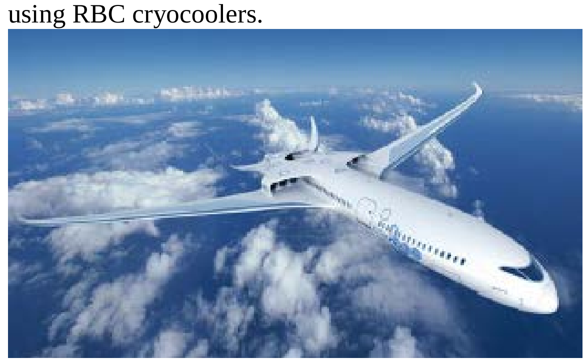

Figure 3 E-Thrust (DEAP) concept aircraft

The second major aircraft concept currently being investigated is the DEAP/E-Thrust concept study shown in Figure 3, led by Airbus Group Innovations and partnered by Rolls-Royce plc and Cranfield University. The DEAP concept airframe is the more traditional tube-and-wing configuration, with the current propulsion configuration specified as two superconducting generators and eight superconducting motor-driven fans, with fans placed along the upper aft fuselage (Berg *et al*, 2015). The total DEAP installed electrical power is between 8 MW and 20 MW. The superconducting material used is MgB_2 throughout, with RBC cryocoolers providing the cooling. The concept also differs from the N3-X concept by stating that liquid methane/LNG would provide an adequate heat sink for the cryocooler, effectively reducing the cryocooler temperature differential and therefore the input power required.

For the purpose of propulsion in this paper, both the DEAP and N3-X aircraft concepts are considered. Figure 4 shows the proposed layout for testing.
The concept used for the analysis carried out in this paper is shown in Figure 3. The half system architecture (Figure 4) includes one superconducting generator, an AC to AC converter, AC distribution network with bus architecture, and a superconducting motor. The efficiency figures for the machines and cables/bus are taken from the DEAP results (Husband *et al*, 2015) while the converter efficiencies are derived from previous NASA studies (Brown, 2011).

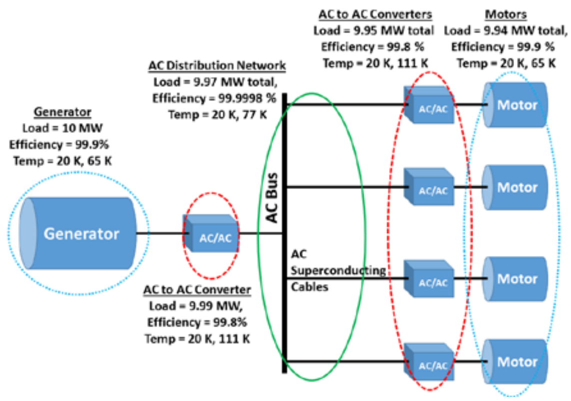

Figure 4 Concept half-system TeDP architecture

All efficiency figures are medium to long term development figures for each component, with the likely TRL 6 target of 2035. All parts apart from the converters are superconducting, with the AC/AC converters assumed to operate optimally at 111 K. The variables are the temperatures of the parts; the machines are assumed to use either MgB_2 or BSCCO, with operational temperatures of 20 K and 65 K respectively. The AC distribution system is assumed to be either MgB_2 or YBCO, with operational temperatures of 20 K and 77 K respectively. It is assumed there are no losses between the machines and converters since they are co-located, and therefore the actual loss is likely to be negligible.

Work is also underway regarding superconducting power distribution without propulsion, or superconducting electrical aircraft (SEA). Cranfield University are presently investigating whether high-power electrical networks that are increasingly being considered for more electric aircraft concepts can offer advantages over conventional electrical networks (Pagonis, 2015). As electrical power levels on board aircraft are increasing with advancements, losses within the electrical system and the corresponding additional weight are becoming proportionally more of a concern. Modern aircraft such as the Boeing 787 have over 1 MW of electrical power within the distribution network, and as heavier hydraulic systems begin to be replaced with linear actuation motors, this power is set to increase.

Studies performed by Cranfield University (Pagonis,

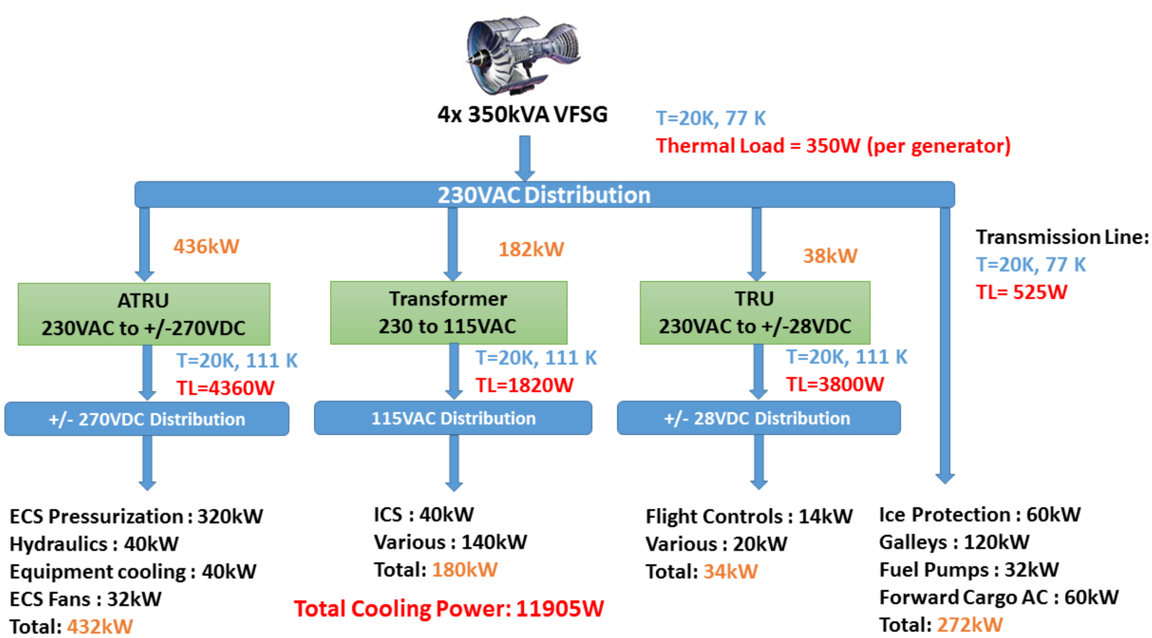

Figure 5 Example SEA network architecture

2015) show that there is likely to be a technical crossover point in technology whereby SEA will be beneficial in both weight and efficiency terms over conventional technology. This paper looks at SEA in a similar way to TeDP, whereby temperatures will be varied among components. An example SEA network is outlined by Pagonis and Malkin (2015). This network is representative of present-day more electric aircraft architectures, such as that of the 787. The configuration shown in Figure 5 shows all loads and losses for an SEA system of 1.4 MW power. As with the TeDP network, the temperatures reflect the materials used, with 20 K, 77 K, and 111 K referring to MgB_2, YBCO, and converter optimum temperature parts respectively. The efficiencies assumed for the SEA concept are more near-term than with the TeDP network. The generator efficiency is assumed to be 99.9%, keeping in line with the DEAP figures. The ATRU and transformer are both set at 99% efficient, and the TRU is set to 90% efficient. The loss in the transmission is assumed at 5 W/m of cabling (Xi *et al*, 2006).

For both the TeDP and SEA concepts, two cooling configurations will be chosen; the minimum number of individual cryocooler stages, and the maximum number up to a ratio of 1:1 concerning components to cryocoolers. The rationale behind this analysis is two-fold; the first is to investigate whether there is any merit besides redundancy in separating cryocoolers for a given concept, particularly when considering mass and input power. The second is to look at the differences in required input power and mass when considering three different temperature architectures, to highlight the effect of design temperature on the overall cryogenic system. Although it is known that cold temperature and both input power and mass have an inverse square relationship (Kittel, 2007), it is not known whether there is a large difference in either parameter by simply changing the cryocooler staging configuration.

The primary focus of this study is temperature management and application of different cooling configurations to suit the network. This study is seen as the entry level study that will kick off a wider design space investigation, whereby temperature-configuration boundaries are eventually established.

Cryogenic Cooling Systems

Previous studies have shown that reverse-Brayton cycle cryocoolers will offer the highest level of performance and reliability based on present-day examples (Palmer and Shehab, 2015). However the configuration options are numerous, with sub-sets of options for each option available. The options in broad terms are:

- Heat sink fluid
- Number of stages per cryocooler
- Ratio of 1st to 2nd stage cryocoolers

Heat sink options are limited to three fluids in previous studies to ambient air, liquid natural gas (LNG) and liquid hydrogen (LH_2). For the purposes of this study, it will be assumed that the heat sink is limited to LNG. The reason for this is that previous studies have highlighted that ambient air is unlikely to result in a cryocooler concept of adequate efficiency (Berg *et al*, 2015). Similarly, LH_2 has been ruled out, however the reason for exclusion is not performance, rather its wider issues of handling such as component embrittlement and storage. LNG presents a compromise between efficiency and availability, and will remain the fixed heat sink for this paper. Furthermore, it is known that many power electronic component operate at optimum efficiency at around the boiling point of LNG, 111 K (Leong, 2011).

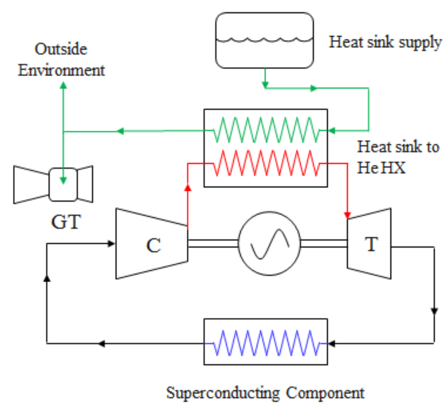

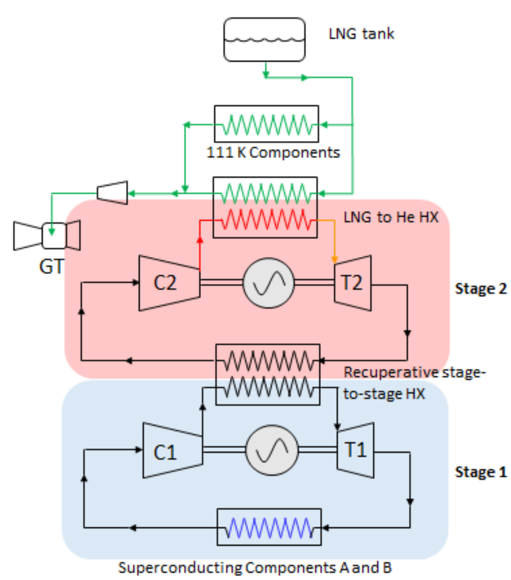

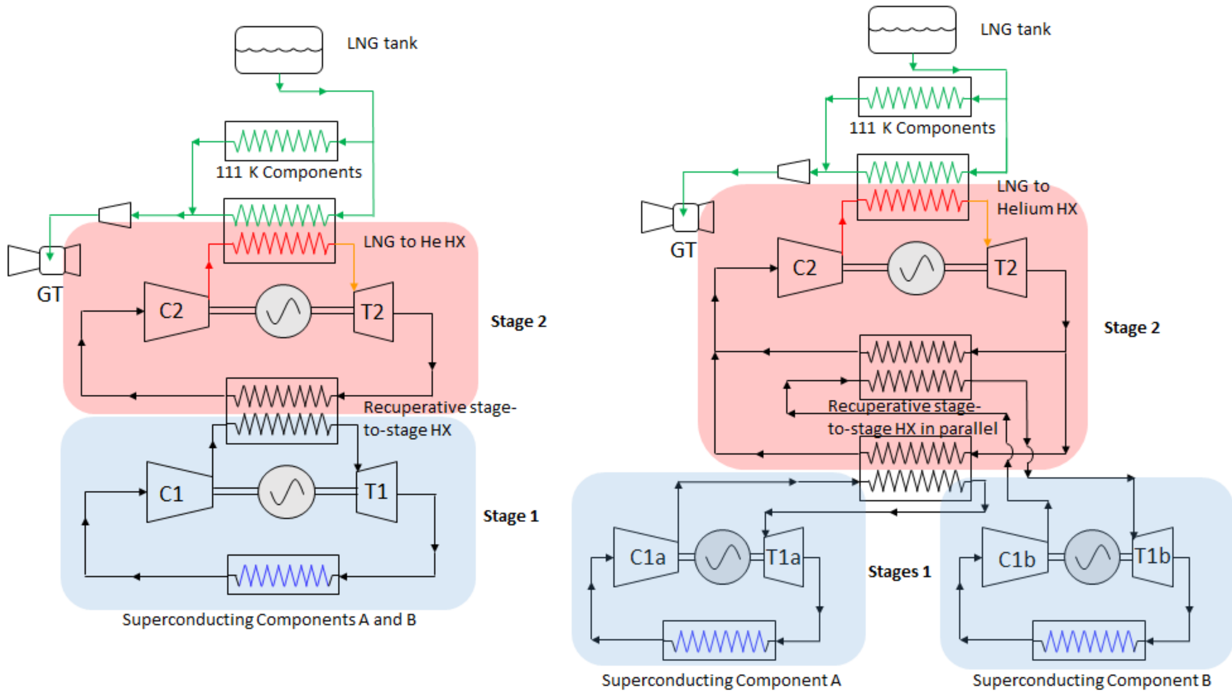

Least Cryocoolers per Component — Most Cryocoolers per Component

Figure 7 Schematic showing basic principles of multi-stage configuration variation

Figure 6 Schematic showing the difference between a single-stage (top) and two-stage (bottom) reverse-Brayton cryocooler

This means that when considering the aircraft system as a closed system (negating the energy required in liquefaction of the LNG on the ground), cooling to 111 K is effectively free. It is known that LNG will have to be re-compressed after it has provided cooling, however for the purposes of this study and to preserve the results of the cryocooler powers and masses, the energy required to do so is ignored.

Finally, number of stages per cryocooler refers to whether a cryocooler is a single-stage, two-stage, or even three-stage design, with the difference depicted in Figure 6. The rationale behind staging of cryocoolers is to reduce the temperature differential per stage, therefore increasing the Carnot efficiency per stage. The caveat to doing this is for every stage is that another set of components is being added, hence overall system weight increases. To date, only single and two-stage designs have been considered for comparison, as three-stage designs are unlikely to meet weight targets. For the purpose of this paper, single and two-stage designs will again be considered, however the load per stage will not be evenly shared. Stage loads are calculated using Equation (1), which splits the overall temperature ratio over both stages evenly. The resulting temperature ratio means that the optimum Carnot cycle for both stages is achieved.

$$\frac{T_{3a}}{T_{4a}} = \sqrt{\frac{T_{3b}}{T_{4a}}} \qquad (1)$$

Where T_{3a} is the 1st stage turbine inlet temperature; T_{3b} is the 2nd stage turbine inlet temperature, and T_{4a} is the 1st stage turbine outlet temperature.

Modelling

The temperature scenarios for both the TeDP and SEA cases are shown in Tables 1 and 2. For each of the three cases, there are two cryogenic system concepts; one with the least possible cryocoolers per component, and the other with a cryocooler per component.

Component	Case 1 Temperature (K)	Case 2 Temperature (K)	Case 3 Temperature (K)
Generator	20	20	65
AC Converter	111	111	111
AC Network	20	77	77
AC Converter	111	111	111
Motor	20	20	65

Table 1 TeDP network temperature cases

For example, the TeDP network consists of one generator, five AC/AC converters, one distribution network (considered a single component due to its relatively modest heat load), and four generators. For the least possible case, the system consists of as many cryocoolers as can least be achieved, which is one for case 1, two for case 2, and two for case 3, to coincide with the number of different temperature set points. For the most possible case, this would change to six cryocoolers for case 1, case 2, and case 3. This is repeated similarly for the SEA network. In all cases, a larger central cryocooler is employed for the second stage. Figure 7 shows the basic schematic differences between the least and most cryocoolers-per-component concepts.

Component	Case 1 Temperature (K)	Case 2 Temperature (K)	Case 3 Temperature (K)
Generator	20	20	77
ATRU	20	111	111
Transformer	20	111	111
TRU	20	111	111
Transmission	20	20	77

Table 2 SEA network temperature cases

This type of layout could prove advantageous; it is known that two-stage cryocoolers per component with multiple second stages is likely to provide redundancy at a cost of weight. However it is not known how pronounced this effect will be if multiple first stages are connected to one central second stage. The loads for each case are calculated using the RBC single stage model developed for project DEAP. The model parametric assumptions used are given in Table 3.

System lowest pressure (bar)	2
Compressor polytropic efficiency (%)	90
Turbine polytropic efficiency (%)	93
Helium specific heat capacity (kJ/kg.K)	5.2
HX pressure drops (%)	5
Cold HX temperature increase (K)	10

Table 3 RBC model assumptions

The intermediate temperatures for the exchange between stages are 49.19 K for concepts requiring cooling to 20 K, and 88.68 K for concepts requiring cooling to 65 K. 77 K concepts are assumed to be single stage in all cases since the temperature differential between 77 K and the 111 K heat sink is adequately small. Cryocooler mass is calculated using the method derived previously (Palmer and Shehab, 2015), shown in (2). The method was derived through surveying RBC systems where masses are known and producing a curve fit.

$$m_{RBC} = 27.5 P_i \mathrm{e}^{-1.225(\log_{10} P_i)} \qquad (2)$$

Where m_{RBC} is cryocooler mass and P_i is the cryocooler input power.

Analysis

Figure 8 shows the TeDP power variation for the least and most cryocooler configurations in all three temperature cases. The results are as expected; there is no variation from the least to most concepts in all three cases. The impact of temperature on the required input power can be clearly seen. Reducing the temperature of the superconducting components by nature of thermodynamics means a much higher required input power; even when considering an LNG heat sink at 111 K.

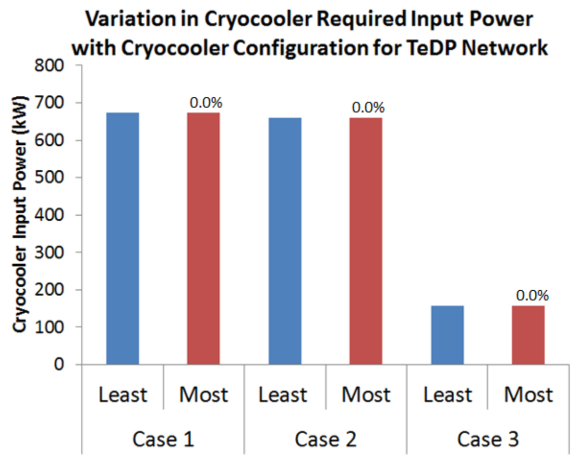

Figure 8 Variation in cryocooler input power with TeDP cryocooler configuration

This shows that future research should consider development of higher temperature superconductors a priority if superconducting TeDP is to be feasible. MgB_2 can offer some advantages at present over BSCCO or YBCO type superconductors however, most notably its manufacturability. Furthermore, Figure 8 highlights the criticality of the superconducting machines over the superconducting network when considering cooling. In case 2 where the distribution network is composed of YBCO superconductor at 77 K, the overall required input power does not drop significantly. As the overall load is comparatively small, the choice of superconductor for the network is essentially free from the cryogenic cooling system constraints. Future research must concentrate on superconducting machine cooling as a priority if TeDP is to be realized.

Figure 9 shows the TeDP concept variation in mass for each case and configuration. As expected the mass is higher for each of the cases where the most cryocooler stages are used. The mass increase for each is significant; all three cases show a mass increase between 35-45%, which in all cases results in mass increases over 200 kg. It is likely that in reality the gap would grow as component level differences in efficiencies are taken into account. It is known that many components when scaled down become less efficient, particularly the compressor and turbines. Parameters such as tip clearances will become a significant issue as cryocoolers are scaled down; subsequent future cryocooler models must begin to reflect this.

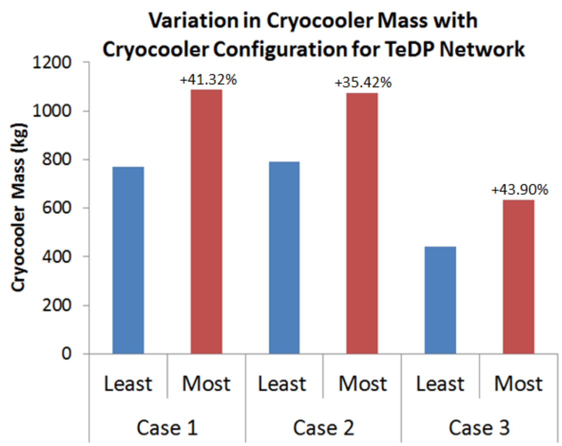

Figure 9 Variation in cryocooler mass with TeDP cryocooler configuration

Figure 10 shows the variation in cryocooler input power with configuration for the SEA network. As with the TeDP network shown in Figure 8, there is no variation between the least and most configurations in all cases.

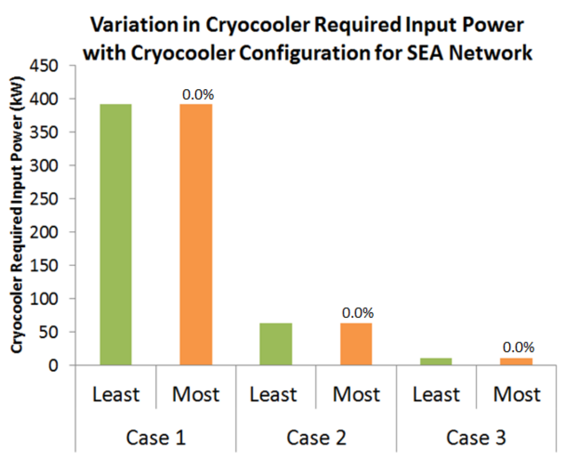

Figure 10 Variation in cryocooler input power with cryocooler configuration for SEA network

Figure 10 highlights a key difference between TeDP and SEA; machines are much less of a concern due to the assumed efficiencies of components. TeDP is assumed to include predicted advancements in technology up to 2035 and beyond. The SEA network example assumes much lower efficiencies that are closer to present-day technology. Power electronics are shown to make up a large percentage of the loss; changing the power electronic component temperature between 20 K and 111 K has resulted in an input power difference of 339 kW between case 1 and 2. Similarly, the difference between case 2 and case 3 is proportional to that of case 1 and 2 at 52 kW. As with the TeDP power levels, temperature has again proved to be the biggest influencing factor in required cryocooler input power. This confirms the need to investigate whether operating temperatures can be raised through using different superconducting materials.

Figure 11 shows the variation in cryocooler mass with cryocooler configuration for the SEA network. As with the TeDP network, the configuration change results in a higher overall cryocooler mass in all three cases. The conclusion of both mass results is that having multiple cryocoolers stages; while potentially advantageous in terms of redundancy, is likely to result in significant mass gain regardless of temperature. Interestingly, the operating temperature difference does not seem to have a large impact on the percentage increase of mass. This suggests that although the mass is affected by temperature change, a determined configuration change will have the same impact on the overall mass regardless of operating temperature. This must be investigated in future research; it is likely that configuration will have an impact in terms of mass, particularly when considering the likely increase in mass that a larger central cryocooler will add in terms of transport tubes. This could be mitigated however through the network architecture; co-locating LNG-cooled cables and cryogenic fluid transport tubes would be a likely solution to mass increases.

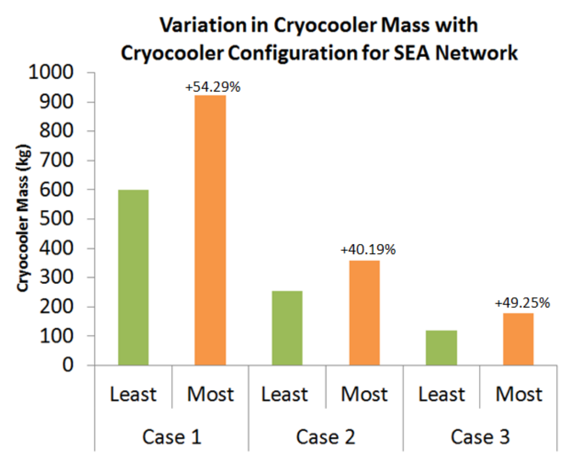

Figure 11 Variation in cryocooler mass with cryocooler configuration for SEA network

Mass increases shown in Figure 11 between the least and most cryocooler cases show that a significant mass increase will result from increasing the number of cryocooler stages. This is due to the nature of the mass-power relationship within cryocoolers; there is a minimum associated mass with cryocoolers, hence as the power levels decrease per first stage, the overall mass does not diminish proportionately. The result of this is the conclusion that as the overall network power increases (and therefore loss), the cryocooler performance per unit mass increases. Figure 9 and Figure 11 both show the increase; hence it is likely that larger aircraft will benefit more from superconducting networks when considering cryogenic cooling systems.

Conclusions

Previous studies have shown that the cryogenic cooling system in future turbo-electric distributed propulsion (TeDP) or superconducting electrical aircraft (SEA) networks is critically sensitive. This paper has investigated how basic cryogenic cooling system choices affect the power required to run the cryocoolers and cryocooler mass for three different temperature cases and two different cryocooler configurations. Results have shown that input power is unaffected by the ratio of cold to warm stages within a given cryogenic cooling system, whereas superconducting component operating temperature is shown to impact input power significantly. This suggests that future work should focus on the type of superconductor used. Superconducting materials such as YBCO and BSCCO are more difficult practically than MgB_2; however the significant increase in required cryocooler input power for MgB_2 should suggest that practical improvements in YBCO and BSCCO should be a research priority. Should advancements be made in this area, both TeDP and SEA will become far more attractive from a performance perspective.

Mass has also been considered; it was found that by increasing the number of stages in a configuration significantly negatively impacted the mass of the cryocoolers in all three temperature cases. The mass increase is attributable to the additional number of components required for separation of stages. While there may be qualitative benefits to separating the cryocooler first stages, the mass per unit cooling power is negatively affected. By increasing the number of stages for a given heat load, cryocoolers are effectively diminishing in power. The decrease in power per stage results in an increase in the proportion of cryocooler mass performing work to the minimum associated mass with having a cryocooler. This result concludes that as aircraft size increases (and therefore loss, provided efficiency remains constant), so does the viability of both TeDP and SEA when considering cryogenics. Given this relationship between cooling power per unit mass, future research projects should include studies for large and very large aircraft.

The final conclusion of this paper is that the models used for DEAP are approaching the limit of their capability. New models are required in order to assess the true impacts of configurationally changes. Future models will need to take into account the differences in component efficiencies when scaling power up or down. The models must also be able to predict mass based on component-level estimations rather than whole system approximations. As the number of stages increases, despite more heat exchangers being required, the number of shared heat exchangers also increases. This must be taken into account in future model iterations for the true impacts of configuration changes to be assessed. Boundaries must be established for configuration choices, which can be used to rapidly iterate performance impacts of future superconducting aerospace networks.

Acknowledgements

The authors gratefully acknowledge the support of Cranfield University, Rolls-Royce plc, Airbus Group Innovations, and the Engineering and Physical Sciences Research Council.

References

Alderman 1. Wright, J., Alderman, J., Berg, F., Dodds, G., Raffaelli, L., Miller, P., Malkin, P., Pagone, E., 2015 “DEAP Final Technical Report”, Internal Document

Berg, F., Palmer, J., Miller, P., Husband, M., and Dodds, G., 2015, “HTS Electrical System for a Distributed Propulsion Aircraft”, *IEEE Transactions on Applied Superconductivity* 25(3): 1-5 June 2015, DOI: 10.1109/TASC.2014.2384731

Brown, G.V., 2011, “Weights and Efficiencies of Electric Components of a Turboelectric Aircraft Propulsion System”, *Presented at the 49th AIAA Aerospace Sciences Meeting* January, Orlando, Florida. AIAA 2011-225

Ekin, J. W., 2006, “Experimental Techniques for Low-Temperature Measurements”, *Oxford University Press*, National Institute of Standards and Technology, pp. 565-575

Felder, J. L., G. V. Brown, and H. D. Kim. 2009. “Turboelectric Distributed Propulsion Engine Cycle Analysis for Hybrid-Wing-Body Aircraft”, In *Proceedings of the 47th Aerospace Sciences Meeting*, Orlando, Florida, USA: American Institute of Aeronautics and Astronautics, January 5-8th 2009.

Green M. W., Schiltgen, B. T., Gibson, A. R., 2012, “Analysis of a Distributed Hybrid Propulsion System with Conventional Electric Machines”, In Proceedings of the 48th AIAA/ASME/SAE/ASEE Joint Propulsion Conference & Exhibit
30 July - 01 August 2012, Atlanta, Georgia

Husband, M., Raffaelli, L., Alderman, J., Berg, F., and Malkin, P., 2015, “Distributed Electrical Aerospace Propulsion”, *Presented More Electric Aircraft (MEA) Conference*, Toulouse, France

Kim, H. D. 2010. “Distributed Propulsion Vehicles”, In *Proceedings of the 27th International Congress of the Aeronautical Sciences*, Nice, France, September 19-24th.

Kittel, P., 2007, “Cryocooler Performance Estimator”, *Cryocoolers*, *Proceedings of the 14th International Cryocooler Conference*, pp. 565

Larbalestier, D., Gurevich, A., Feldmann, D.M., Polyanskii, A., 2001, “High-T_c superconducting materials for electric power applications”, Nature Journal, vol. 414, pp. 368-377

Leong, K.K., 2011, “Utilising Power Devices Below 100 K to Achieve Ultra-low Power Losses”, PhD Thesis, University of Warwick

Malkin, P., Pagonis, M., 2014, “Superconducting Electric Power Systems for Hybrid Electric Aircraft”, Aircraft Engineering and Aerospace Technology Journal: An International Journal, Vol. 86, iss. 6, pp. 515 – 518

Pagonis, M., 2015, “Electrical Power Aspects of Distributed Propulsion Systems in Turbo-electric Powered Aircraft” (temporary title), PhD thesis (to be published), Cranfield University

Malkin, P. and Pagonis M., 2015, “Future Energy Solutions for Hybrid-Electric Powered Aircraft”, *Presented at ISABE 2015* (to be published)

Palmer, J., and Shehab, E., 2015, “Modelling of Cryogenic Cooling System Design Concepts for Superconducting Aircraft Propulsion”, *Submitted to the IET Electrical Systems in Transportation Journal*, Awaiting publication

Xi, H.X., Gong, W.Z., Zhang, Y., Bi, Y.F., Ding, H.K., Wen, H., Hou, B., and Xin, Y., 2006, “China’s 33.5m, 35kV/2kA HTS AC power cable’s operation in power grid”, *Physica C: Superconductivity*, vol. 445-448, pg. 1054-1057